High-Sensitivity Demodulation of Fiber-Optic Acoustic Emission Sensor Using Self-Injection Locked Diode Laser

Farzia Karim, Abu Farzan Mitul, Bohan Zhou, and Ming Han

***Abstract*—We demonstrate the use of a self-injection locked distributed feedback (DFB) diode laser for high-sensitivity detection of acoustic emission (AE) using a fiber-coil Fabry-Perot interferometer (FPI) sensor. The FPI AE sensor is formed by two weak fiber Bragg gratings on the ends of a long span of coiled fiber, resulting in dense sinusoidal fringes in its reflection spectrum that allows the use of a modified phase-generated carrier demodulation method. The demodulation method does not require agile tuning capability of the laser, which makes the self-injection locked laser particularly attractive for the application. Experimental results indicate that the self-injection locked laser increases the signal-to-noise ratio by ∼33 dB compared with the free-running DFB laser. We studied the mode-hopping and laser instability of the self-injection locked laser and their effect on the demodulated signal and found that a mode hopping event causes an abrupt change in the laser intensity after the resonator inside the feedback loop. It manifests itself as a short transient signal in the output of the AE sensor system. With the identification of the mode-hopping events, the associated spurious signal can be identified and discarded in the signal processing without causing significant disruption to the sensor system. Experiment shows that the frequency of locked lasers could oscillate during unstable operations. The fundamental frequency is determined by the time delay of the feedback light and is typically much larger than the AE frequency. Therefore, the laser frequency oscillations have no negative effect on the performance of the sensor system. Finally, we show that the frequency of mode-hopping occurrence is related to the length of the feedback loop and reducing the loop length can effectively reduce the frequency of mode-hopping occurrence.**

***Index Terms*—Fiber Bragg gratings, laser self-injection locking, Fabry-Perot interferometer, phase-generated carrier demodulation, ultrasonic sensors, fiber-optic sensors, structural health monitoring.**

I. Introduction

MANY damage-related structural changes, such as crack initiation, crack growth, and fiber breakage, are accompanied by a sudden release of stress energy, leading to the generation of transient elastic waves typically in the frequency range of 20 kHz to 1 MHz. These waves are called acoustic emission (AE) and its detection has been widely used for structural health monitoring. Traditionally, piezoelectric sensors are used for AE detection. Recently, fiber-optic AE sensors, especially those based on fiber Bragg gratings (FBGs), have become an attractive alternative and are being intensively studied because they provide several advantages such as light weight, small size, corrosion resistance, multiplexing capabilities, and immunity to electromagnetic interference [1], [2]. Because of the required detection speed, these sensors are typically demodulated by the edge filter detection technique, in which the wavelength of a tunable laser is locked on the slope of the spectral features of the sensor to convert AE-induced spectral shift to the intensity variations of the reflected laser light [3]–[5]. Detection sensitivity (characterized by the minimum detectable wavelength shift) is a key performance parameter of fiber-optic AE sensors. Previous effort to improve the detection sensitivity has been focused on increasing the slope of the spectral feature through FBG-based optical resonators such as chirped FBG Fabry–Perot interferometers (FPIs) [6] or π-phase-shifted FBGs [7], [8], which can generate narrow resonant features with spectral width on the order of 1 pm in the 1550 nm wavelength window. As the spectral slope increases, the noise of the system is ultimately dominated by the laser frequency noise, which is converted to laser intensity variations by the spectral slope and shows up as the noise at the output of the photodetector. Locking of the laser wavelength on a narrow spectral feature also requires agile wavelength tuning capability of the laser. Therefore, a tunable laser with minimum frequency noise is critical for these advanced sensors to reach their potential of high-sensitivity AE detection. Existing low frequency noise lasers for fiber-optic AE sensors are mostly external cavity diode lasers. They have a long cavity length and thus provide a high-quality factor of the laser cavity, rendering excellent frequency noise performance. However, the bulk size, the complexity of the laser cavity, the stringent optical alignment requirements, and the high cost limit their use in practical applications. Self-injection locking of a diode laser [9] is a powerful yet simple laser frequency noise reduction technique in which a small portion of the laser is injected back to laser diode after it goes through an external resonator. The external resonator converts the frequency fluctuations of the laser into amplitude fluctuations, which are in turn converted back into frequency fluctuations through the

Manuscript received 12 July 2022; accepted 15 July 2022. Date of publication 21 July 2022; date of current version 29 July 2022. This work was supported by the Office of Naval Research under Grants N000141812273, N000142112273, and N000141812597. *(Corresponding author: Ming Han.)*

The authors are with the Department of Electrical and Computer Engineering, Michigan State University, East Lansing, MI 48824 USA (e-mail: karimfa1@msu.edu; mitulabu@msu.edu; zhouboha@msu.edu; mhan@egr.msu.edu).

Digital Object Identifier 10.1109/JPHOT.2022.3192806

amplitude-phase coupling in the laser diode. A proper feedback phase adjustment can cause destructive interference of this frequency fluctuations with the original laser frequency fluctuation and provide a reduced laser frequency noise [10]. It has been demonstrated that self-injection locking can be performed on commercial fiber-pigtailed distributed feedback (DFB) diode lasers to achieve sub-Hz Lorentzian linewidth through a fiber feedback loop constructed from fiber-optic circulators and fiber-optic resonators such as FBG-FPIs or fiber-ring resonators (for comparison, linewidths of free-running DFB diode lasers are typically a few MHz) [11]–[14]. Due to the excellent noise performance and straightforward implementation, fiber-pigtailed lasers under self-injection locking have been studied as light sources for fiber-optic sensor systems whose performance is sensitive to laser frequency noises such as phase-sensitive optical time-domain reflectometry systems and fiber-optic gyroscopes [15]–[18]. However, the long optical feedback length makes the lasers prone to mode-hopping. There have been reported attempts at suppressing mode-hopping by light polarization control and using more compact resonator [16], [17], but no detailed characterization of mode-hopping and the associated laser instability has been reported. In addition, little work has been reported on using self-injection locked lasers in fiber-optic AE or ultrasonic sensor systems due to the challenges induced by the lack of the agile wavelength tuning capability of a self-injection locked laser.

In this work, we demonstrate the use of a self-injection locked DFB diode laser for high-sensitivity demodulation of a fiber-coil FPI AE sensor formed by two weak FBGs on the ends of a long span of coiled fiber [19]. Taking advantage of the dense sinusoidal fringes of the sensor reflection spectrum, we developed a modified phase-generated carrier (PGC) demodulation method that does not require agile tuning capability of the laser [20]. Experimental results indicate that, compared with the free running DFB laser, the self-injection locked laser increases the signal-to-noise ratio (SNR) by ∼33 dB compared with that of the free-running DFB laser. We also studied the effect of the mode-hopping events of the self-injection locked laser on the demodulated signal. We found that mode-hopping is often associated with laser frequency oscillations that could last for a length of the order of seconds. The mode-hopping event causes an abrupt change in the laser intensity after the resonator inside the feedback loop. It manifests itself as a short transient signal in the output of the AE sensor system. With the identification of the mode-hopping events, the associated spurious signal can be identified and discarded in the signal processing without causing significant disruption to the sensor system. We also found that laser frequency oscillation can also occur spontaneously without the mode-hopping. The spectrum of the laser frequency oscillations shows narrow peaks at the fundamental frequency determined by the feedback loop length and its harmonics. Because these frequency components are much higher than the bandwidth of the fiber-optic AE sensor system, they have no effect on the performance of the sensor system. Finally, we show that the frequency of mode-hopping is highly related to the length of the feedback loop and reducing the loop length can effectively reduce the frequency of mode-hopping.

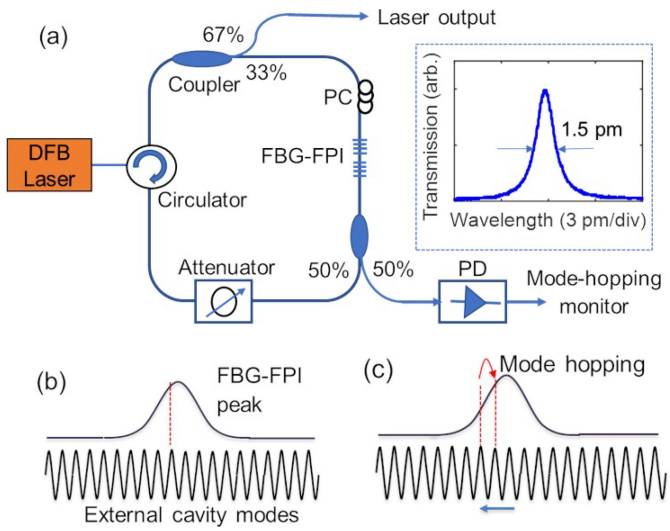

Fig. 1. (a) Schematic of self-injection locked DFB laser locking setup. PD: photodetector, PC: polarization controller. Inset: Spectrum of the transmission peak of an FBG-FPI in the feedback loop. Schematic illustration of (b) dense external cavity modes with respect to the FBG-FPI transmission spectrum and (c) mode-hopping event of the self-injection locked laser.

II. Experiment

A. Self-Injection Locked DFB Diode Laser

The self-injection locked DFB diode laser is similar to the one described in [21] and is schematically shown in Fig. 1(a). The light source is a DFB diode laser without an integrated isolator at ∼1545 nm. The optical feedback path included the fiber pigtail of the DFB laser and a fiber loop. The light from the DFB laser was coupled to the fiber loop through a circulator and traveled through a high-finesse FBG-FPI functioning as the locking resonator before it was injected back to the laser diode through the same circulator. Other components included in the fiber loop were a polarization controller (PC) for aligning the laser polarization with one of the principal axes of the FBG-FPI, an attenuator for adjusting the feedback coefficient, and two fiber-optic couplers. The feedback level needs to be adjusted to an appropriate level. It should be large enough to the induced locking. We also found that too much feedback tends to induce more frequent episodes of laser instability. The 33:67 coupler before the PC was used to couple out a portion of the light in the cavity as the output of the self-injection locked laser that would be sent to the fiber-optic AE sensor system. The 50:50 coupler after the FBG-FPI was used for monitoring the mode-hopping events as described below. The locking resonator is an FBG-FPI consisting of two identical 3-mm long uniform FBGs at ∼1545 nm separated by a 4-mm long fiber. Its transmission spectrum had several resonant peaks with the narrowest one having a 3-dB linewidth of 1.5 pm (shown in the inset of Fig. 1(a)) that was used for self-injection locking.

The front facet of the laser diode and the feedback path including the fiber pigtail and the fiber loop formed an external cavity that was weakly coupled to the DFB laser cavity in the laser system. The feedback path length ranged from a few meters to over 20 meters by including jump cables in the fiber loop.

As schematically shown in Fig. 1(b), the long feedback path length results in dense external cavity modes over a broad wavelength range. When the appropriate feedback coefficient is obtained by tuning the attenuator, the laser is then locked to one of the external cavity modes around the transmission peak of the FBG-FPI. Ambient perturbations such as temperature variations and vibrations to the fiber feedback path can cause drift of the external cavity modes and changes of the relative positions of the external cavity modes and the resonator peak. For example, the thermos-optic coefficient of silica is $dn/dT = \sim 1 \times 10^{-5}$. A relative temperature change of 0.1 °C between the FPG-FPI and the fiber loop would cause a 1 pm wavelength drift between the external cavity mode and the FBG-FPI peak, which is significant considering the 1.5 pm spectral width of the FBG-FPI peak. As schematically shown in Fig. 1(c), when the external mode to which the laser is locked drifted away from the resonator peak, the optical loss of the mode-hopping increases and may eventually jump to the neighboring external cavity mode with smaller loss, resulting in a mode-hopping event. Accompanied with the mode-hopping event is an abrupt change of the light intensity after the resonator, which can be monitored by a photodetector.

B. Fiber-Optic AE Sensor and Modified PGC Demodulation

We demonstrated the application of self-injection locked laser for AE detection using a low-finesse FPI sensor demodulated by a modified PGC method [20]. The sensor was made from a pair of weak FBGs at the ends of a fiber coil made from a span of ∼40-cm long optical fiber, leading to approximately sinusoidal fringes with a free-spectral range of ∼2 pm and the fringe profile determined by the FBG reflection spectrum. The outer and inner loop diameter of the fiber coil sensor was 10 mm and 8 mm, respectively. The schematic of the fiber-coil sensor and its reflection spectrum, as well as the measured fine fringes of the sensor, are shown in Fig. 2(a). Details on the fabrication and characterization of the sensor can be found in Ref. [19]. As shown in Fig. 2(b), the coiled region of the sensor was then glued on an aluminum plate (91 cm × 66 cm × 1 mm) for testing. AE signals were simulated by a piezo transducer glued on the aluminum plate around 2 cm away from the center of fiber coil sensor which was driven by a sinusoidal signal of 150 kHz, 10 V peak-to-peak, 4 cycle burst (10 ms period) from a function generator. Since only the coiled fiber region (without FBGs) was bonded on the surface of a structure, surface strain including that caused by the AE signal induced changes to the phase of the sensor fringes and the spectral profile of the fringes remained unchanged.

The modified PGC method allowed to extract the AE signal encoded as the phase modulation with good linearity and high sensitivity and regardless of the laser wavelength with respect to the sensor fringes. Detailed description of the demodulation method is described in Ref. [20]. For convenience, the method is briefly introduced here. The light intensity reflected from the low-finesse FPI may be written as $I = A + B\cos[\phi_0 + \Delta\phi(t)]$, where A and B are constants related to the laser power and the fringe visibility, ϕ_0 is a quasi-static phase

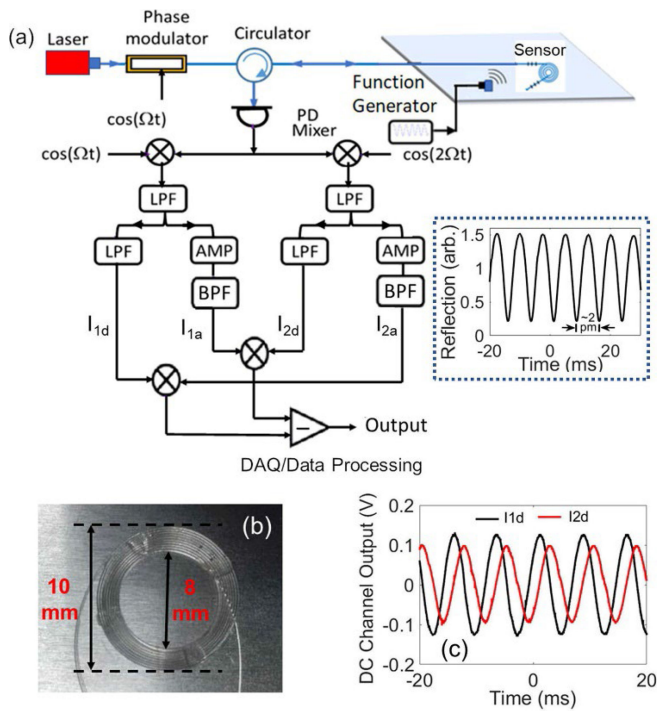

Fig. 2. (a) Schematic of a modified PGC demodulation method for fiber coil sensor. PD: photodetector, AMP: amplifier, DAQ: data acquisition, LPF: low pass filter, BPF: band pass filter. Inset: reflection spectrum of fiber-coil sensor measured by a wavelength-scanning laser. (b) An image of a fiber coil sensor installed on an aluminum plate. (c) Two dc channel outputs while the laser wavelength was scanned linearly with time.

term including the laser wavelength drift and environmental effect, and $\Delta\phi(t)$ is an ac term proportional to the AE signal being detected. As shown in Fig. 2(a), the phase of the laser is modulated with a sinusoidal function with a frequency of Ω using an electro-optic phase modulator to generate the carrier signals. The light intensity reflected from the sensor, detected by a photodetector, then contains an in-phase signal, $\cos[\phi_0 + \Delta\phi(t)]$ and a quadrature signal, $\sin[\phi_0 + \Delta\phi(t)]$, modulated by carrier signals with frequencies of the even and odd multiples of Ω, respectively. The terms at carrier frequencies Ω and 2Ω, or $-2BJ_1(C)\sin[\phi_0 + \Delta\phi(t)]$ and $-2BJ_2(C)\cos[\phi_0 + \Delta\phi(t)]$, where J_1 and J_2 are, respectively, the first and second-order Bessel function of the first kind and C is a constant related to the phase modulation depth and the modulation frequency which can be obtained by mixing the output from the photodetector with sinusoidal signals at the same frequency and applying a low pass filter with a bandwidth covering the highest frequency of signal of interest. Recognizing AE-induced phase changes are small or $\Delta\phi(t) \ll 1$, we can apply the following approximations and break the in-phase and quadrature signals each into a quasi-dc component and an ac component that is linearly proportional to $\Delta\phi(t)$:

$$\sin\left[\phi_0 + \Delta\phi\left(t\right)\right] \approx \sin\phi_0 + \cos\phi_0 \Delta\phi\left(t\right)$$

and

$$\cos\left[\phi_0 + \Delta\phi\left(t\right)\right] \approx \cos\phi_0 - \sin\phi_0 \Delta\phi\left(t\right).$$

The dc components can be obtained by applying a low-pass filter and ac components can be separated by a bandpass filter and an amplifier. Then we obtain the following four signals:

$$I_{1d}\ (t) = -2BJ_1\,(C)\sin\phi_0 \tag{1a}$$

$$I_{1a}\ (t) = -2BGJ_1\,(C)\cos\phi_0\Delta\phi\,(t) \tag{1b}$$

$$I_{2d}\ (t) = -2BJ_2\,(C)\cos\phi_0 \tag{1c}$$

$$I_{2a}\ (t) = 2BGJ_2\,(C)\sin\phi_0\Delta\phi\,(t) \tag{1d}$$

where G is the gain of the amplifier. Then $\Delta\phi(t)$, with the AE signal encoded in it, can be extracted with good linearity and independent on ϕ_0 through the following algebraic operation:

$$I_{1a}\,(t)\,I_{2d}\,(t) - I_{1d}\,(t)\,I_{2a}\ (t) = 4GB^2J_1\,(C)\,J_2\,(C)\,\Delta\phi\,(t)\,. \tag{2}$$

In our experiment, the phase modulator was a high-speed (10 GHz) lithium niobate electro-optic phase modulator (Model: 2942, Covega), driven by a 130 MHz sinusoidal waveform generated from a function generator and an RF amplifier. The terms at the carrier frequencies were then obtained by properly mixing the output of PD with sinusoidal waves at the fundamental and second-order harmonic of the carrier signal and a 500 kHz low pass filter (LPF). After the low-pass filter, the signal of interest, which was ultrasound, was then separated and amplified by a 40 dB amplifier and bandpass filter in the frequency range of 50-500 kHz. The bandwidth was selected to cover most of the frequency components of AE signals for crack detection in structural health monitoring applications. For quasi-dc channels, another 25 kHz LPF was applied following the 500 kHz LPF. The cut-off frequency of quasi-dc channel needs to cover the frequency range of the unwanted signals that can cause the shift of the operating point such as environmental perturbations. The four signals (2 quasi-dc and 2 ac) as represented by Eqs. (1a)–(1d) were then recorded by an oscilloscope or a data acquisition (DAQ) with a sampling rate of 2 MS/s for storage in a computer, where the operation in (2) was performed to obtain the output of the system. We verified that the demodulation setup could generate the in-phase and quadrature signals using the carrier signal. For this purpose, we employed a tunable laser whose wavelength was modulated by a triangular wave and recorded two quasi-dc terms, $I_{1d},\ I_{2d}$ as shown in Fig. 2(c), which shows the system produced two sinusoidal waveforms with quadrature phase relationship.

III. Results

A. Comparison of SNRs With Self-Injection Locked Laser and Free-Running Laser

We connected the DFB sensor system in self injection-locked mode and in free-running mode to the demodulation system. The feedback loop length of the self-injection locked laser was approximately 9 m. The responses of both configurations to the simulated AE signal generated by the piezo transducer on the aluminum plate are shown in Fig. 3(a) and (c), respectively. It shows that both configurations yield similar overall ultrasonic response with similar peak-to-peak signal values around 0.43 V^2. It also clearly demonstrates that, the self-injection locked

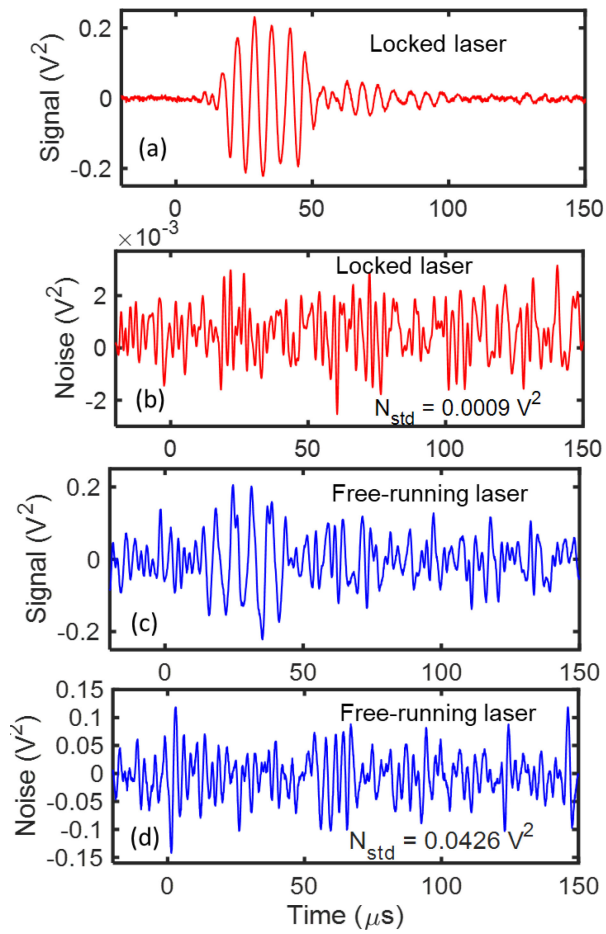

Fig. 3. (a) Ultrasonic response and (b) noise provided by the system with self-injection locked DFB laser system. (c) ultrasonic response and (d) system noise with the same laser in free-running mode.

mode provides much smaller noise as compared to the free-running mode of DFB laser. The noise with the free-running DFB laser is dominated by the laser frequency noise of the laser [22]. The sensor system cannot distinguish between the laser frequency variations and the AE-induced wavelength shift of the sensor. To characterize the noise performance of the sensor system more accurately in these two configurations, we turned off the piezo transducer so that there was no simulated AE signal, and the system outputs absent of the AE signal for the self-injection locked mode and the free-running mode of DFB laser are shown in Fig. 3(b) and (d), respectively. The standard deviations of noises are 9.0×10^{-4} V^2 and 4.3×10^{-2} V^2, respectively, for these two modes. Using the peak-to-peak response and standard deviations for calculating the SNR, we found that the self-injection-locked DFB laser (SNR = 53.6 dB) provides a much better SNR which is ~33 dB larger than that the of free-running DFB laser (SNR = 20.0 dB).

We also characterized the noise improvement for self-injection locked lasers with different feedback loop length in comparison to free-running laser. A longer feedback loop may further reduce the laser frequency noise [23]. However, in the current system, the noise with the self-injection locked laser was dominated by the noise from the photodetectors and the

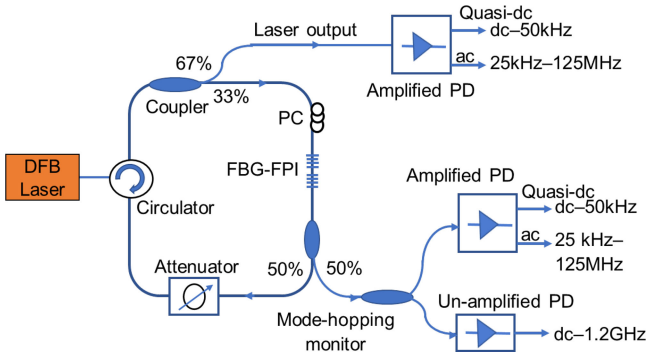

Fig. 4. Experimental setup to study mode-hopping and the instability of the self-injection locked laser.

electronics of the sensor system. We found that increasing the loop length to 14 m did not cause significant changes to the SNR performance.

B. Characterization of Mode-Hopping and Laser Frequency Oscillations

As discussed in Section II, environmental perturbations could cause a relative drift of the external cavity mode with respect to the resonator wavelength of the self-injection locked laser that leads to mode-hopping. It is expected that mode-hopping will result in a step change of laser frequency. We found that the laser wavelength is typically locked to the slope of the resonator, where the wavelength change is converted to intensity variations of the light passing through the resonator. Therefore, the occurrence of mode-hopping can be identified by monitoring the intensity of the light after it passes through the resonator in the feedback loop.

We used various photodetectors to observe the signal, including a broadband dc-coupled um-amplified photodetector (Model: DET01CFC, Thorlabs) with a bandwidth from dc to 1.2 GHz to observe the overall signal and an amplified photodetector (Model: 1811, Newport) with both an ac (25 kHz–125 MHz) output and a quasi-dc (dc-50 kHz) output. As shown in Fig. 4, the amplified photodetector was also applied to the laser output port to monitor the power of the light before passing through the resonator.

We first studied the signals from the mode-hopping monitoring port of the laser system. Fig. 5(a) shows the output from the un-amplified photodetector when a mode-hopping event occurred. It shows that the mode-hopping resulted in a jump in the signal level followed by unstable laser operation as indicated by the rapid variations of the output that lasted for less than 1 s. Due to the presence of the instability, it is difficult to accurately characterize the transient time of the mode-hopping. The variations are more clearly visible at the ac output of the amplified photodetector (Fig. 5(b)). The quasi-dc output of the photodetector with a 50 kHz bandwidth (Fig. 5(c)) only shows a step change of the output, which can be attributed to the mode-hopping, but is absent of the variations associated with the laser instability, indicating that the variations have no frequency components below at least 50 kHz. Fig. 5(d) shows

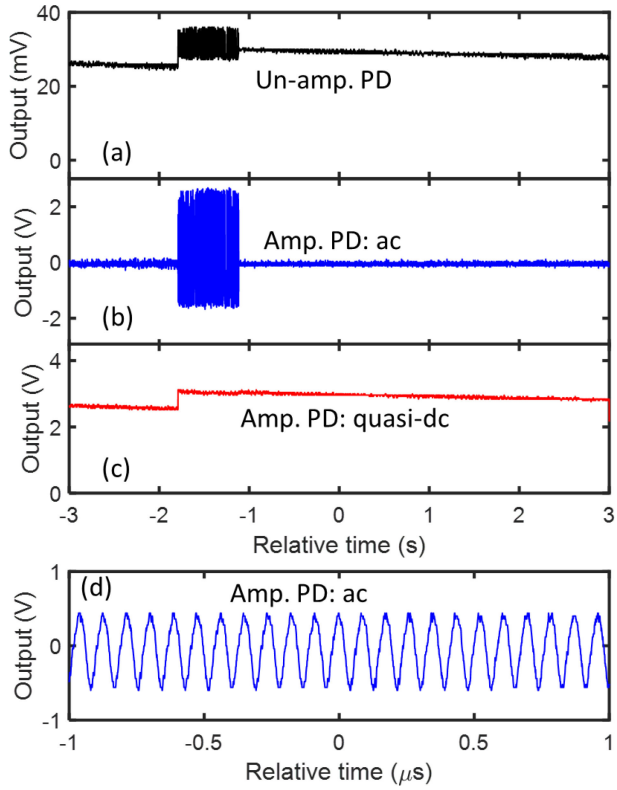

Fig. 5. (a)–(c) Signals from the photodetectors (PDs) connected to the mode-hopping port of the self-injection locked laser. (d) Oscillation signals from the ac output of the amplified PD when the laser is in unstable operation.

the details of the variations at another instance when the laser instability was observed. It indicates that the variations have a periodic structure with a period of 86 ns, corresponding to a fundamental frequency of ∼11 MHz. We found that the period of the oscillations corresponds to the time delay of the feedback light from a single trip of the feedback loop. Note that, the shape of the oscillations may deviate from a sinusoidal shape. In those cases, the signal may contain strong components at higher-order harmonic frequencies.

For the case shown in Fig. 5, the laser become unstable following the mode hopping. We also observed that the instabilities can precede the mode-hopping or occur spontaneously without mode-hopping. For example, in Fig. 6(a), a mode-hopping event indicated by the step change in the quasi-dc output of the amplified photodetector is preceded by the variations indicative of the laser instability recorded from the ac port of the amplified photodetector. In another example shown in Fig. 6(b), the quasi-dc output has no step changes, indicating the absence of mode-hopping. However, the laser instability is clearly visible in the ac output. We note that, the laser instability lasted for various lengths on the order of seconds. The variations recorded by the photodetectors were caused by the laser frequency oscillations rather than the laser intensity variations at the output of the locked DFB laser. It is proved by the experiment in which we simultaneously monitored the output from the mode-hopping monitoring port (laser intensity after the resonator) and the laser output port (laser intensity before the resonator) as shown in

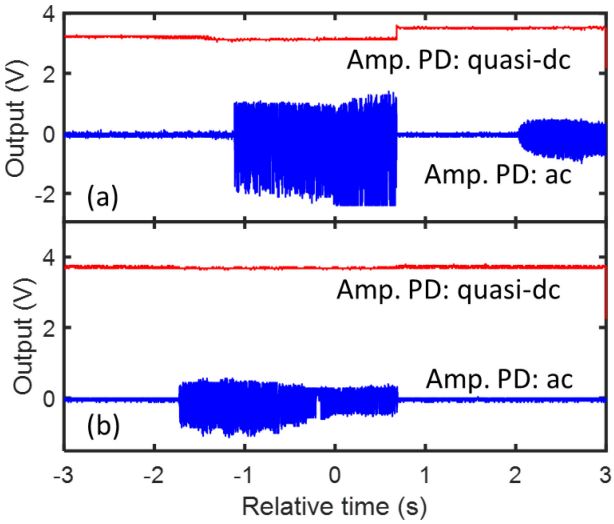

Fig. 6. (a) and (b) are the two instances in which the laser instability (a) occurs preceding the mode-hopping and (b) occurs spontaneously without mode-hopping.

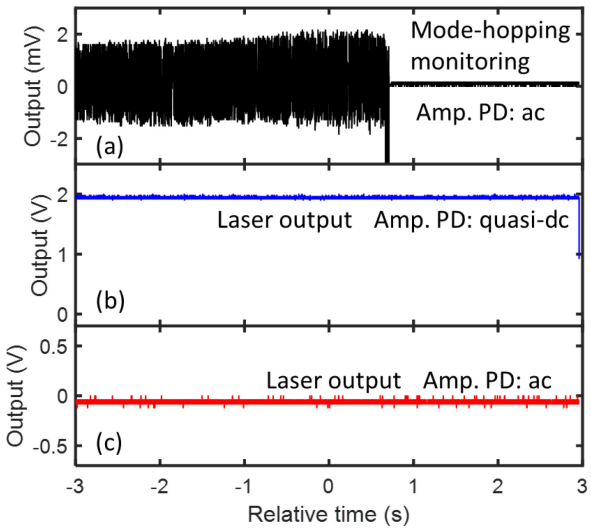

Fig. 7. (a) Instability recorded from amplified PD connected to mode-hopping monitoring port of self-injection locked laser after resonator. (b)–(c) are signals from the amplified PDs connected to the laser output port before resonator.

Fig. 4. The results are shown in Fig. 7, where Fig. 7(a) is the ac output of the amplified photodetector at the mode-hopping monitoring port and Fig. 7(b) and (c) are respectively the quasi-dc and ac outputs of another amplified photodetector at the laser output port. Fig. 7(a) shows that the laser operation was unstable before relative time $t \approx 0.8$ s and became stable afterwards. Between these two laser states, no changes were observed in either the quasi-dc output or the ac output for the laser output ports. Therefore, the variations observed in Fig. 7(a) must have come from the laser frequency variations that were converted to the laser intensity variations at the spectral slope of the resonator. Similar frequency oscillations have also been observed in self-injection locked semiconductor lasers with long free-space coupled feedback loops [24], [25].

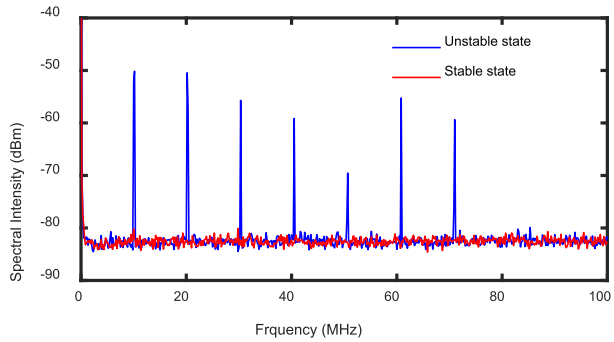

Fig. 8. Spectra of the signals from the ac output of the amplified PD connected to the mode-hopping monitoring port when the laser is in unstable operation (blue) and in stable operation (red).

We measured and compared the electronic spectrum of the signal from the ac output of the amplified photodetector connected to the mode-hopping monitoring port when the self-injection locked laser was in stable state and unstable state. Fig. 8 shows an example of the measured spectra. It verifies the conclusions from the time-domain analysis. The laser under stable state shows a flat baseline in the bandwidth of the detector. The unstable operation of the laser results in oscillations with a fundamental frequency of $\sim$11 MHz. Several strong harmonic frequency components are also present. However, the noise level remained unchanged between the stable and unstable operation for frequencies other than at these discrete values.

Finally, we note that, due to the presence of the instability and the short time scale of the dynamics, it is difficult to accurately capture the temporal evolution as the locked laser frequency jumps from one mode to the other mode during a mode-hopping event. Relaxation oscillation (RO) is involved in establishing a lasing mode in the process. The RO frequency of a DFB laser typically is $>$1 GHz. As a result, the transition time of the mode hopping may be on the order of 1 ns, which is much faster than the time scale of the AE signal ($<$1 MHz) in the application studied here.

C. *Effect of Mode-Hopping of Self-Injection Locked Laser on System Response*

In the laboratory environment, we observed that mode hopping occurred infrequently. To study the effect of mode hopping on the system response, we intentionally perturbed the fiber loop by bringing an incandescent light close to the FBG-FPI region to slightly heat the fiber loop, which led to more frequent mode-hopping events. The four channels in the demodulation system, I_{1d}, I_{2d}, I_{1c}, and I_{2c}, as shown in Fig. 2(a) as well as the mode-hopping monitor signal were continuously recorded. In the meantime, simulated AE signals were continuously generated with a repetition rate of 100 Hz during the data acquisition process.

Fig. 9(a) shows the evolution of the recorded signals as well as the calculated AE response according to (2) over a period of $\sim$1.5 s. Noted that, proper multiplication factors and offset values are added in Fig. 9 for clarity. The mode-hopping events

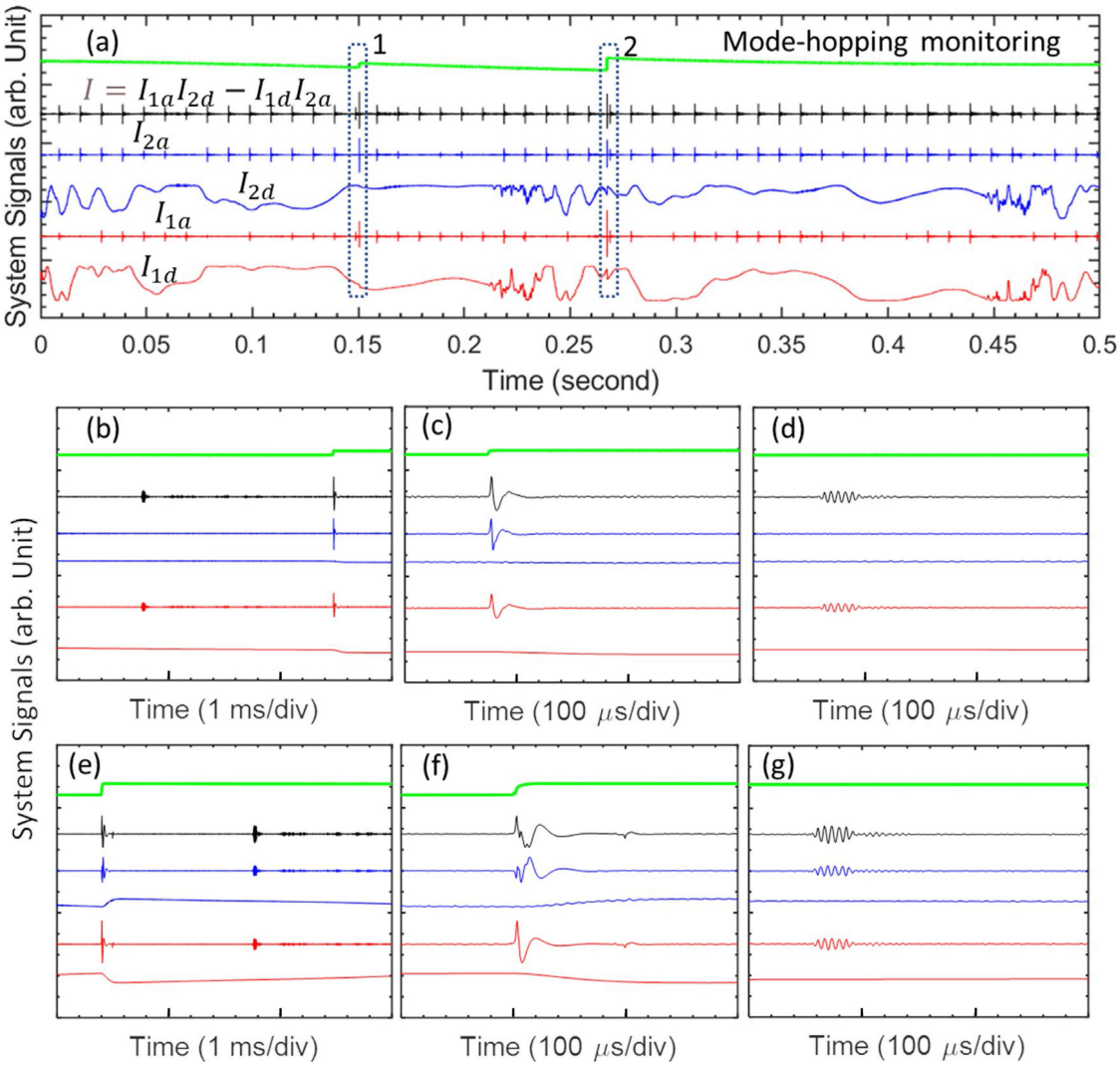

Fig. 9. (a) Four-channel response with mode-hopping signal and overall ultrasonic response of the AE sensor system. (b) Enlarged view of Fig. 9(a) around the first mode-hopping event showing both the signal due to mode-hopping with more details shown in (c) and the response to the simulated AE signal with more details shown in (d); (e) Enlarged view of Fig. 9(a) around the second mode-hopping event showing both the signal due to the mode-hopping with more details shown in (f) and the response to the simulated AE signal with more details shown in (g).

are indicated by the jumps in the light intensity after the locking resonator recorded as the mode-hopping monitoring signal (green curve in Fig. 9(a)). It is seen that two mode-hopping events occurred during the 1.5 s period of recording. The variations of the two quasi-dc signals, I_{1d} and I_{2d}, show that the operating point changed during the data recording. The overall response of the system shows relatively uniform response to the simulated AE signal with a repetition rate of 100 Hz. Fig. 9(b) is the enlarged view of the signal around the time when the first mode-hopping occurred at around 2 seconds marked by a sharp increase in the intensity of the mode-hopping monitoring signal. A closer examination reveals that the mode-hopping event was also accompanied by step changes in the two quasi-dc components. It also shows that, preceding the mode-hopping, a simulated AE signal generated by the piezo actuator arrived at the sensor and was detected. A close-up view of the system signals at the time of the mode-hopping are shown in Fig. 9(c). The two ac components signal, I_{1c} and I_{2c}, and the overall system output, I, show transient responses to the mode-hopping. The waveform shows an oscillation that only lasted less than two cycles and resembles the step response of a heavily damped bandpass filter. The pattern of the transient responses is different from the responses to the simulated AE signal, which is shown in Fig. 9(d). The response to the AE signal shows a main wave packet with many cycles typical to AE signals. Therefore, we can conclude that the signals shown in Fig. 9(c) were caused by the mode-hopping of the self-injection locked DFB diode laser but not by the AE signal.

The system response to the second mode-hopping has similar characteristics to the first mode-hopping. As shown in Fig. 9(e), a step change in the mode-hopping signal indicates the occurrence of the second mode-hopping event and a simulated AE pulse arrived at the sensor about 1.5 ms after the mode-hopping event and was detected by the sensor. Note that, the mode-hopping signal

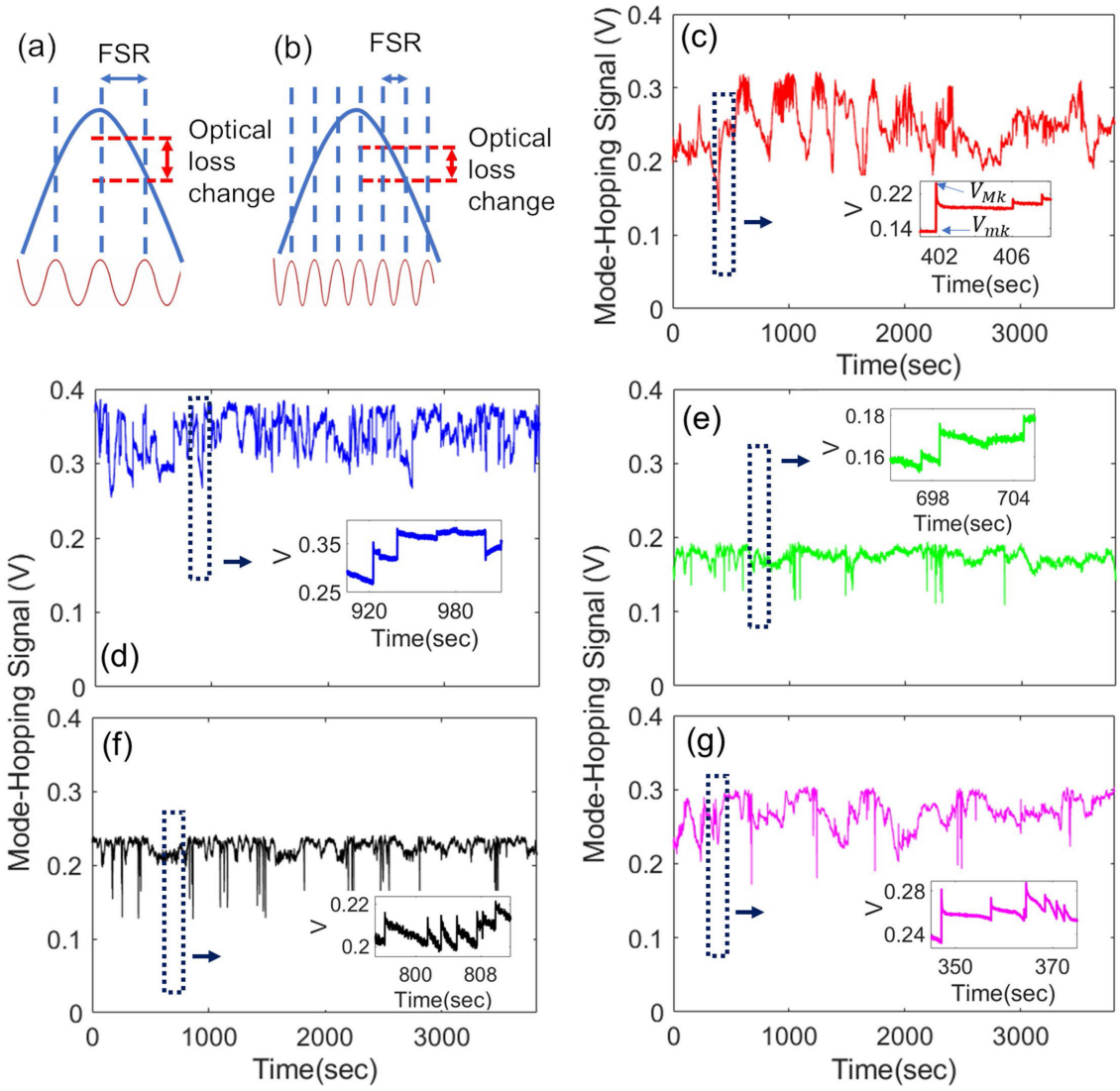

Fig. 10. Schematic illustration of (a) shorter loop length with large FSR provides less frequent mode-hopping with larger change in optical loss (b) longer loop length with small FSR provides more frequent mode-hopping with smaller change in optical loss. Mode-hopping jumps of self-injection locked laser for fiber ring loop length of (c) 7 m, (d) 9 m, (e) 11 m, (f) 14 m, (g) 24 m. Insets: Enlarged view of mode-hopping for different loop lengths as marked by a box and an arrow.

shows a larger step change compared to the first mode-hopping. The change in the step size is related to the wavelength position of the locking point relative to the spectrum of FBG-FPI in the feedback loop (see Fig. 10(a)) below. Fig. 9(f) is the detailed views of the transient response due to the mode-hopping and the transient lasted about 120 μs. The mode-hopping did not affect the detection of the simulated AE signal as shown in Fig. 9(g). We note that, transient response to mode-hopping last around 100 μs, which is likely determined by the detection bandwidth of the sensor system. In addition, a mode-hopping event can be reliably identified. Therefore, the transient signals due to the mode-hopping events can be reliably identified and removed from the overall signal. Note that according to the results shown in Section III-B, the laser could experience unstable operations that can accompany the mode-hopping events or occur spontaneously. Because they have distinct frequencies above the frequency range of the AE signal, they do not affect the operation of the sensor system.

D. Occurrence Frequencies of Mode-Hopping

As mentioned earlier, mode-hopping does not occur frequently for the self-injection locked DFB diode laser under laboratory environment. The laser can maintain stable operation over periods ranging from a few seconds to a few minutes. The experiment in Section III were performed when external perturbation was intentionally introduced to the fiber feedback loop to induce more frequent mode-hopping of the locked laser. Here, we studied the mode-hopping events in the laboratory environment with no intentional perturbations. We paid attention to the occurrence frequency of mode-hopping events and the level of the intensity jump in the mode-hopping monitoring signal from the mode-hopping events in relation to the length of the self-injection locked feedback loop. As shown in Fig. 10(a), the laser was locked to one of the external cavity modes close to the resonant peak of the FBG-FPI. The interval of the external cavity modes is determined by the free-spectral range (FSR) of external

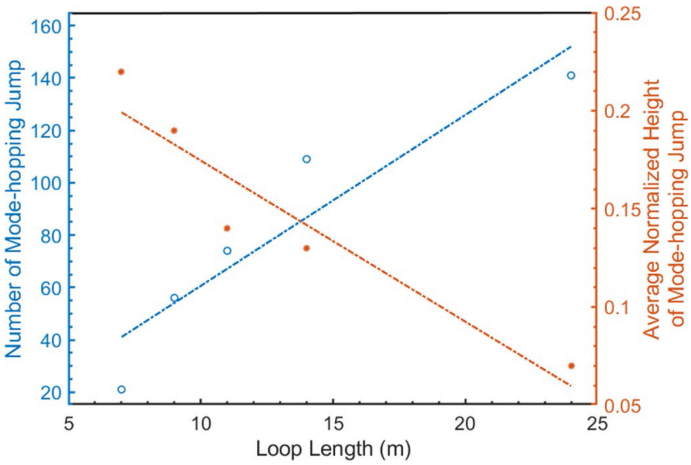

Fig. 11. Relationship of loop length with number of mode-hopping and average normalized height of mode-hopping jump.

cavity (feedback loop) given by $\mathrm{FSR} = \lambda^2/2nL$, where λ is the wavelength of operation, n is the refractive index of the fiber, and L is the length of the feedback loop. As schematically shown in Fig. 10(a), shorter loop length provides a larger FSR and on average, a larger change in the optical loss between neighboring external modes, resulting in less frequent mode-hopping jump with on average, larger mode-hopping jump height because of the large distance between the external cavity modes. On the other hand, longer loop provides smaller FSR with denser sinusoidal fringes resulting in more frequent mode-hopping occurs with smaller jump levels due to the smaller distance between the external cavity modes, as schematically shown in Fig. 10(b). We varied the fiber length of the feedback loop from 7 m to 24 m by including the fiber patch cables of various lengths in the feedback loop. For each loop length, we monitored the naturally occurring mode-hopping events of self-injection locked DFB laser by recording the mode-hopping monitoring signals for 1 hour. Fig. 10(c)-(g) show the results for loop lengths about 7 m, 9 m, 11 m, 14 m, and 24 m, respectively. The enlarged view of mode-hopping jumps for different loop lengths are also shown in the in-sets of Fig. 10(c)-(g) as marked by a box and an arrow. In addition, we studied the effect of feedback loop length on mode-hopping occurrence frequency by counting the number of the jumps in the mode-hopping events. We have also estimated the average normalized height of mode-hopping jumps, $\bar{S}$, for different loop lengths of the self-injection locked DFB diode laser according to the following definition:

$$\bar{S} = \frac{1}{N}\sum_{k=1}^{N}\frac{V_{Mk} - V_{mk}}{(V_{Mk} + V_{mk})/2}, \tag{3}$$

where, N is the number of mode-hopping jumps during the period of monitoring, and V_{mk} and V_{Mk} are respectively, the signal level right before and after the jumping, as schematically shown in the inset of Fig. 10(c).

Fig. 11 shows the number of the recorded mode-hopping events and the average normalized height of mode-hopping jumps for different loop lengths, as well as the linear fittings of the data points. It demonstrates that, the number of mode-hopping increases with the increasing of loop-length. On the other hand, average normalized height of mode-hopping jump decreases with the increasing of loop length and number of mode-hopping. Both show a relatively good linear relationship with the feedback loop length. Therefore, number of mode-hopping is inversely proportional to the mode-hopping height.

The results show that, in general, shorter loop lengths provided smaller number of mode-hopping events with larger jump heights. Therefore, reducing the feedback loop length can effectively reduce the number of mode-hopping events in a self-injection locked DFB diode laser. In the laboratory environment, 141 mode-hopping events were registered for self-injection locked laser with the longest fiber loop length (24 m). On average, a mode-hopping event occurs every 25 seconds. As shown in Section III, the spurious transient signals from a mode-hopping event only lasted ~100 μs. Therefore, the disruption to the AE sensor system caused by removing the spurious signal from the mode-hopping event of the self-injection locked laser is likely insignificant and negligible.

It needs to be stressed that the experiment was performed in a laboratory environment. Larger perturbations that can be experienced in the field may cause more frequent mode- hopping and even unlocking of the laser if the discrepancy between the free-running laser wavelength and the resonator wavelength becomes large. As the minimum feedback loop length may still be on the order of meters due to the use of fiber-pigtailed lasers and other fiber-pigtailed components, the laser system is expected to be prone to environmental perturbations and likely needs to be packaged and protected for practical applications in the field. Active approaches, e.g., controlling the drift of the external cavity mode through a fiber stretcher, to minimize the mode-hopping could also be considered.

IV. Conclusion

A self-injection locked DFB diode laser AE sensor system has been demonstrated using a fiber optic interferometric sensor through a modified PGC demodulation method. The self-injection locked DFB diode laser had a narrow notch filter of 1.5 pm linewidth which served as a locking resonator in a fiber ring feedback loop. We locked the laser wavelength to an external cavity mode on the spectral slope of the filter. The self-injection locked DFB diode laser ultrasonic sensor system proposed in this work provided ~33 dB higher SNR than that of a DFB diode laser in free-running mode. We also studied the mode-hopping and laser instability as well as their effect on the performance of the sensor system. Experimental results demonstrates that, the mode-hopping of self-injection locked DFB laser induced transient responses that lasted only around 100 μs. The mode-hopping induced response can be identified and removed with negligible impact on the detection of the AE signal. The laser instable operation characterized by the laser frequency oscillations can accompany the mode-hopping or occur spontaneously without mode-hopping. We found that the oscillations have spectral components at discrete frequencies much higher than the AE frequency and do not affect the

performance of the sensor performance. In addition, experimental results show that, we could also reduce the occurrence frequency of mode-hopping events by reducing the loop length and thus increasing the spectral spacing of the external cavity modes.

ACKNOWLEDGMENT

The authors would like to thank our former lab members, Dr. Yupeng Zhu (currently with Applied Materials, Santa Clara, California, USA) and Dr. Guigen Liu (currently with Harvard Medical School, Boston, Massachusetts, USA) for their assistance in constructing the experimental setup.

REFERENCES

[1] M. Meo, " 6 - Acoustic emission sensors for assessing and monitoring civil infrastructures," *Sensor Technol. Civil Infrastructures*, vol. 1, pp. 159–178, Jan. 2014.

[2] C. B. Scruby, "An introduction to acoustic emission," *J. Phys. E: Sci. Instrum.*, vol. 20, no. 8, Aug. 1987, Art. no. 946.

[3] D. C. Betz, G. Thursby, B. Culshaw, and W. J. Staszewski, "Acousto-ultrasonic sensing using fiber Bragg gratings," *Smart Mater. Struct.*, vol. 12, no. 1, Jan. 2003, Art. no. 122.

[4] Q. Wu, Y. Okabe, and F. Yu, "Ultrasonic structural health monitoring using fiber Bragg grating," *Sensors*, vol. 18, no. 10, Oct. 2018, Art. no. 3395.

[5] M. Majumder, T. K. Gangopadhyay, A. K. Chakraborty, K. Dasgupta, and D. K. Bhattacharya, "Fibre Bragg gratings in structural health monitoring—Present status and applications," *Sensors Actuators A: Phys.*, vol. 147, no. 1, pp. 150–164, Sep. 2008.

[6] Q. Zhang, Y. Zhu, X. Luo, G. Liu, and M. Han, "Acoustic emission sensor system using a chirped fiber-Bragg-grating Fabry–Perot interferometer and smart feedback control," *Opt. Lett.*, vol. 42, no. 3, pp. 631–634, Feb. 2017.

[7] G. Liu and M. Han, "Wavelength locking of a diode laser to the maximal slope of a π-phase-shifted fiber Bragg grating for acoustic emission detection," *IEEE Sensors J.*, vol. 18, no. 22, pp. 9257–9262, Nov. 2018.

[8] T. Liu and M. Han, "Analysis of π -phase-shifted fiber Bragg gratings for ultrasonic detection," *IEEE Sensors J.*, vol. 12, no. 7, pp. 2368–2373, Jul. 2012.

[9] B. Dahmani, L. Hollberg, and R. Drullinger, "Frequency stabilization of semiconductor lasers by resonant optical feedback," *Opt. Lett.*, vol. 12, no. 11, pp. 876–878, Nov. 1987.

[10] H. Li and N. B. Abraham, "Analysis of the noise spectra of a laser diode with optical feedback from a high-finesse resonator," *IEEE J. Quantum Electron.*, vol. 25, no. 8, pp. 1782–1793, Aug. 1989.

[11] W. Lewoczko-Adamczyk *et al.*, "Ultra-narrow linewidth DFB-laser with optical feedback from a monolithic confocal Fabry-Perot cavity," *Opt. Exp.*, vol. 23, no. 8, pp. 9705–9709, Apr. 2015.

[12] D. Xu *et al.*, "Subkilohertz linewidth reduction of a DFB diode laser using self-injection locking with a fiber Bragg grating Fabry-Perot cavity," *Opt. Exp.*, vol. 24, no. 15, pp. 17406–17415, Jul. 2016.

[13] Y. Zhao and C. Shu, "Single-mode operation characteristics of a self-injection seeded Fabry-Perot laser diode with distributed feedback from a fiber grating," *IEEE Photon. Technol. Lett.*, vol. 9, no. 11, pp. 1436–1438, Nov. 1997.

[14] A. A. Savchenkov, A. B. Matsko, D. Seidel, L. Maleki, V. S. Ilchenko, and W. Liang, "Whispering-gallery-mode-resonator-based ultranarrow linewidth external-cavity semiconductor laser," *Opt. Lett.*, vol. 35, no. 16, pp. 2822–2824, Aug. 2010.

[15] J. L. Bueno Escobedo *et al.*, "Self-injection locking of the DFB laser through an external ring fiber cavity: Application for phase sensitive OTDR acoustic sensor," *Results Phys.*, vol. 7, pp. 641–643, Jan. 2017.

[16] J. L. Bueno Escobedo *et al.*, "Distributed measurements of vibration frequency using phase-OTDR with a DFB laser self-stabilized through PM fiber ring cavity," *Results Phys.*, vol. 12, pp. 1840–1842, Mar. 2019.

[17] M. Kong, R. Zhang, X. Li, X. Zhu, and Z. Zhao, "Using DFB laser self-injection locked to an optical waveguide ring resonator as a light source of Φ-OTDR," *Appl. Opt.*, vol. 60, no. 31, pp. 9769–9773, Nov. 2021.

[18] J. Geng, L. Yang, S. Zhao, and Y. Zhang, "Resonant micro-optical gyro based on self-injection locking," *Opt. Exp.*, vol. 28, no. 22, pp. 32907–32915, Oct. 2020.

[19] G. Liu, Y. Zhu, Q. Sheng, and M. Han, "Polarization-insensitive, omni-directional fiber-optic ultrasonic sensor with quadrature demodulation," *Opt. Lett.*, vol. 45, no. 15, pp. 4164–4167, Aug. 2020.

[20] F. Karim, Y. Zhu, Y. Zhu, and M. Han, "Modified phase-generated carrier demodulation of fiber-optic interferometric ultrasound sensors," *Opt. Exp.*, vol. 29, no. 16, pp. 25011–25021, Aug. 2021.

[21] Y. Zhu, L. Hu, Z. Liu, and M. Han, "Ultrasensitive ultrasound etection using an intracavity phase-shifted fiber Bragg grating in a self-injection-locked diode laser," *Opt. Lett.*, vol. 44, no. 22, pp. 5525–5528, Nov. 2019.

[22] L. Hu and M. Han, "Reduction of laser frequency noise and intensity noise in phase-shifted fiber Bragg grating acoustic-emission sensor system," *IEEE Sensors J.*, vol. 17, no. 15, pp. 4820–4825, Aug. 2017.

[23] C. Henry, "Theory of spontaneous emission noise in open resonators and its application to lasers and optical amplifiers," *J. Lightw. Technol.*, vol. 4, no. 3, pp. 288–297, Mar. 1986.

[24] A. P. A. Fischer, M. Yousefi, D. Lenstra, M. W. Carter, and G. Vemuri, "Filtered optical feedback induced frequency dynamics in semiconductor lasers," *Phys. Rev. Lett.*, vol. 92, no. 2, 2004, Art. no. 023901.

[25] H. Erzgräber, B. Krauskopf, D. Lenstra, A. P. A. Fischer, and G. Vemuri, "Frequency versus relaxation oscillations in a semiconductor laser with coherent filtered optical feedback," *Phys. Rev. E - Statist. Nonlinear, Soft Matter Phys.*, vol. 73, no. 5, May 2006, Art. no. 055201.